Materials Science and Engineering A 399 (2005) 26–32

MATERIALS SCIENCE & ENGINEERING A

www.elsevier.com/locate/msea

An investigation of springback stresses in AISI-1010 deep drawn cups

Thomas Gnaeupel-Herold [a,b,*], Timothy Foecke [c], Henry J. Prask [b], Richard J. Fields [c]

[a] *University of Maryland, Department of Materials and Nuclear Engineering, College Park, MD 20742-2115, USA*
[b] *National Institute of Standards and Technology, Center for Neutron Research, 100 Bureau Dr. Stop 8562, Gaithersburg, MD 20899, USA*
[c] *National Institute of Standards and Technology, Metallurgy Division, Gaithersburg, MD 20899, USA*

Abstract

The residual stresses created by deep drawing of AISI-1010 cups were investigated by means of neutron diffraction. The wall thickness of the cups was below 3.0 mm, for which 8–10 through-thickness measurements were conducted. It was found that the axial, and tangential stress profiles are similar to what is expected from a bending–unbending operation, but it also exhibits a strong dependence on the axial and, to a minor extent, on the circumferential position. The strong axial stress dependence reflects the effect of stretching while the weaker circumferential stress variations are due to sheet anisotropy. We also found that the thermal relief of cold work in the initial AISI-1010 cold rolled blank has no discernable effect both on the residual stresses and the springback.
© 2005 Elsevier B.V. All rights reserved.

Keywords: Springback; Deep drawing; Residual stress

1. Introduction

Springback is the elastic shape change of sheet metal after forming and removal from the die. In the automotive industry, the poor predictability of springback has always been a problem but it was somewhat alleviated by the use of rather thick walled, low strength steels. Due to the increasing need for weight reduction there is a major shift underway to use thinner high strength steels and aluminum alloys. In both cases, these materials exhibit larger springback magnitudes, thus making an accurate prediction all the more necessary in order to avoid costly re-design of the stamping tool.

Current modeling efforts concentrate on the development of 3D computer models to predict stress, strain, and fracture in sheet metal, with the goal of a significant reduction in tool design time. For the first stage of springback modeling with the accompanying measurements, deep drawn cups are chosen as a generic part. They are easily produced and provide a simple measure of springback with a large magnitude displacement. Furthermore, the formed cups exhibit many features found in production parts, such as large biaxial strains, thickness variations, and texture.

Residual stresses in the cup exist because different locations in the cup have accumulated different magnitudes of plastic strain. These stresses are key for the modeling of springback because their integral over the wall thickness yields a non-zero bending moment and thus a shape change.

Most of the stress-related experimental and theoretical work done on deep drawn cups has focused on the actual value of the springback, which is measured as the opening of a ring cut from the center section of the cup and subsequently split open [1–7]. The difficulty in modeling the opening as an integral effect is that a multitude of stress distributions can produce the same opening, thus making it more difficult to optimize the computer model in a way that it reproduces the actual stresses in the cup wall. However, even with the extensive research done on deep drawn cups, only few publications have dealt with the measurement of springback stresses. These include X-ray surface measurements [1], an early neutron diffraction measurement done at low spatial resolution [3], and a very recent synchrotron diffraction study on a Al-6022 cup [7]. While the latter has provided detailed insight into the axial and tangential stresses in the cup wall, questions remain about the dependence of the stresses on the axial and circumferential position. It is also long established that external processes and material parameters such as the strength of the material, sheet thickness, pre-strain and flow control

* Corresponding author. Tel.: +1 301 975 5380; fax: +1 301 921 9847.
E-mail address: tg-h@nist.gov (T. Gnaeupel-Herold).

0921-5093/$ – see front matter © 2005 Elsevier B.V. All rights reserved.
doi:10.1016/j.msea.2005.02.017

measures have a large effect on the springback. However, more data are needed to clarify how the stress distributions are affected by these parameters.

In this work, we examine in detail the stresses in the cup rings before and after cutting operations, i.e. after cutting the cup into rings and after splitting the ring. In order to study the effect of pre-strain a second cup was made from a blank where the cold work from cold rolling was removed by annealing.

2. Experimental

2.1. Forming

The cups were made in the Forming Laboratory of the NIST Metallurgy Division using a hydraulic deep drawing machine with 500 kN capacity. The AISI-1010 blanks were circular disks of 200 mm diameter and 3.00 mm thickness. The diameter of the die bore was 110 mm with a rim radius of 10 mm. The stamping tool had a diameter of 100 mm with an edge radius of 10 mm. The depth of the cups was 55 mm. Vegetable oil was used as a lubricant. The forming rate was constant at 5 mm/s, and the hold-down load was constant at 90 kN. A detailed description of the forming process can be found in Ref. [8].

2.2. Neutron diffraction measurements

All strain measurements were done using the BT8 Residual Stress Diffractometer at the NIST Center for Neutron Research using a wavelength of 2.26 Å and the (0 1 1) reflection. The (0 1 1) reflection is best suitable for this experiment because of the texture-induced raise in scattered neutron intensity in the axial, radial and hoop directions. Because of the specimen geometry involved, and in order to ensure the best possible spatial resolution, two different gauge volumes were defined with apertures for the incident beam (width × height) and the diffracted beam (opening). A schematic of the neutron beam geometry and the respective specimen orientations is shown in Fig. 1. Both for the tangential and the axial strain component a gage volume of 3 mm × 0.5 mm × 3 mm ($w \times h \times o$) was used while for the radial direction a gage volume of 0.5 mm × 7 mm × 0.5 mm was defined. This way, the depth resolution for each of the three directions was 0.5 mm. Data were collected in eight steps of 0.4 mm through-thickness, in five steps of 45° around the circumference in the midsection, and at three different axial locations. The d-spacings both the innermost and the outermost point of each scan were affected by partial illumination, i.e. the gauge volume was half immersed in the sample. This effect is equivalent to a specimen displacement, and it was corrected by rotating the specimen by 180° for which the shift of the d-spacing is opposite. For small displacements as in our case the correction is obtained by the average of both measurements.

Two cups were investigated. The first cup was made from a blank in the as-received condition. After EDM cutting three rings from the cups, stress measurements were made both for the intact and split rings in the mid-ring at positions (0°, 45°, 90°, 135° and 180°) and at the (0°) position in the top-ring and the bottom-ring. The dimensions of the rings and measurement locations are illustrated in Fig. 11.

In order to relieve internal stresses from cold rolling, the blank for the second cup was annealed for 40 min at 630 °C in an argon atmosphere. At this temperature, the yield strength of a mild steel such as AISI-1010 is <30 MPa [9] and virtually all cold work is removed after 40 min. Then, a cup was drawn from this blank using the same forming conditions as for the cup made from the as-received blank. Diffraction measurements on the second were done on the mid-ring at the (0°) position.

The low thickness of the cup wall permitted the application of the $\sigma_{\text{radial}} \equiv 0$ boundary condition. This increases the overall accuracy of the stress calculations because $\sigma_{\text{radial}} \equiv 0$ is generally very well fulfilled for such a thin-walled structure, and the condition applies for every point on the surface. The use of this condition removes the influence of d_0-variations. It also simplifies the stress equations to

$$\sigma_{\text{hoop}} = \frac{d_{\text{hoop}} - d_{\text{radial}}}{d_0} \times \frac{E_{hkl}}{1 + \nu_{hkl}}$$
$$\sigma_{\text{axial}} = \frac{d_{\text{axial}} - d_{\text{radial}}}{d_0} \times \frac{E_{hkl}}{1 + \nu_{hkl}} \quad (1)$$

where d_{radial}, d_{hoop} and d_{axial} are the measured d-spacings, d_0 is the reference d-spacing (for which the average of all d-spacings was chosen) and E_{hkl}, ν_{hkl} are the diffraction elastic constants calculated according to [10]. The Eq. (1) are insensitive to the choice of d_0 because the variations of measured d-spacings are well below 1%. The uncertainties of the stresses in Figs. 4–6, 8–10 were obtained from the standard deviations of the fitted peak positions.

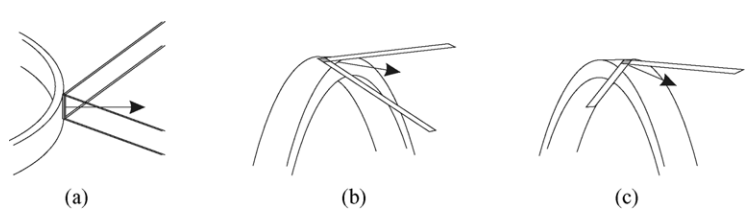

Fig. 1. Neutron beam and specimen orientation for the radial (a), axial (b) and hoop (c) measurements. The arrows point out the direction of the scattering vector.

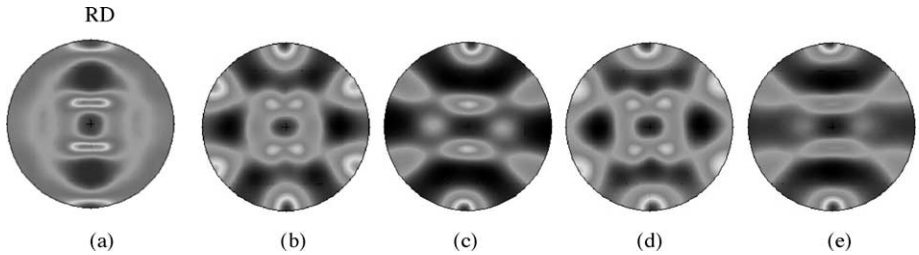

Fig. 2. (0 1 1) pole figures for the initial blank (a), the 45° location (b) and the 135° location (c) of the mid-ring, the tensile sample after 35% deformation in the TD direction (d) and the tensile sample after 40% deformation in the RD direction.

In order to identify the initial rolling direction (RD) and transverse direction (TD) of the blank (0 1 1)-pole figures were measured every 45° on the cup wall and on tensile samples cut from a second blank. The texture measurements on the cup showed distinctive differences between pole figures at locations at 45°, 90° and 135°. Then, tensile samples cut from an undeformed blank in RD and TD orientation were subjected to a uniaxial strain of 35% and 40%, and pole figures were measured again. The pole figure of the deformed RD specimen was very similar to the one at the 135° location, and the pole figure of the deformed TD specimen was similarly close to the pole figure at the 45° location on the cup wall. This way both RD and TD could be clearly identified as shown in Fig. 2.

2.3. Thickness measurements

Thickness measurements were done in 10° steps on all the three rings using a dial gage with ±0.005 mm accuracy by measuring the variation of the roundness both on the inside and the outside of a ring, and normalizing both measurements to the thickness at one location. This procedure yields the radii on the inside and on the outside. The subtraction from one another provides the thickness distribution.

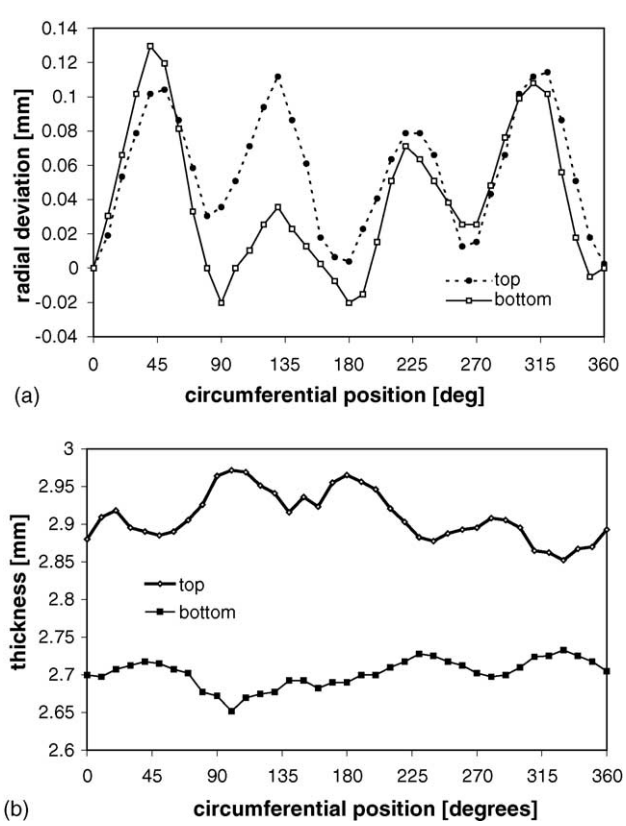

Fig. 3. Surface roundness profiles (a) and thickness profiles (b) for the top and bottom rings of the cup made from the as-rolled blank. The thickness of the original blank was 3.00 mm.

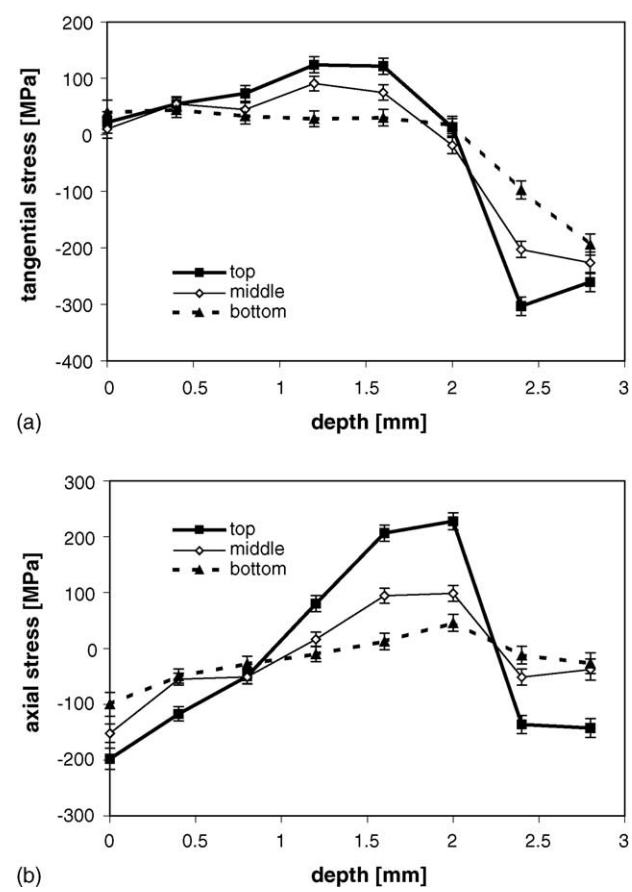

Fig. 4. Tangential (a) and axial (b) stresses in the intact rings at the "0°" position at different axial positions (see Fig. 11). The *x*-axis (depth) starts at the outer surface.

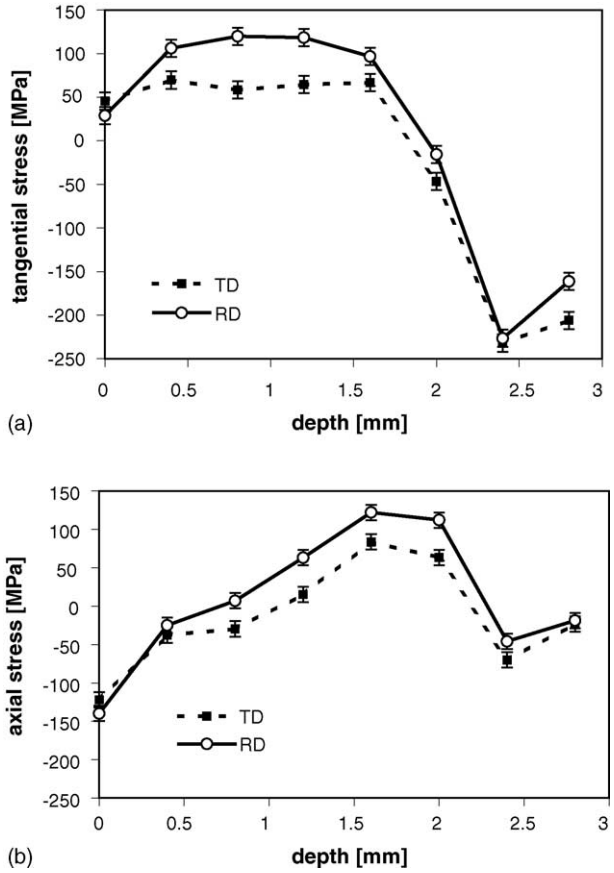

Fig. 5. Tangential (a) and axial (b) stresses in the intact mid-ring measured at the original transverse direction (TD) and at the rolling direction (RD). The *x*-axis (depth) starts at the outer surface.

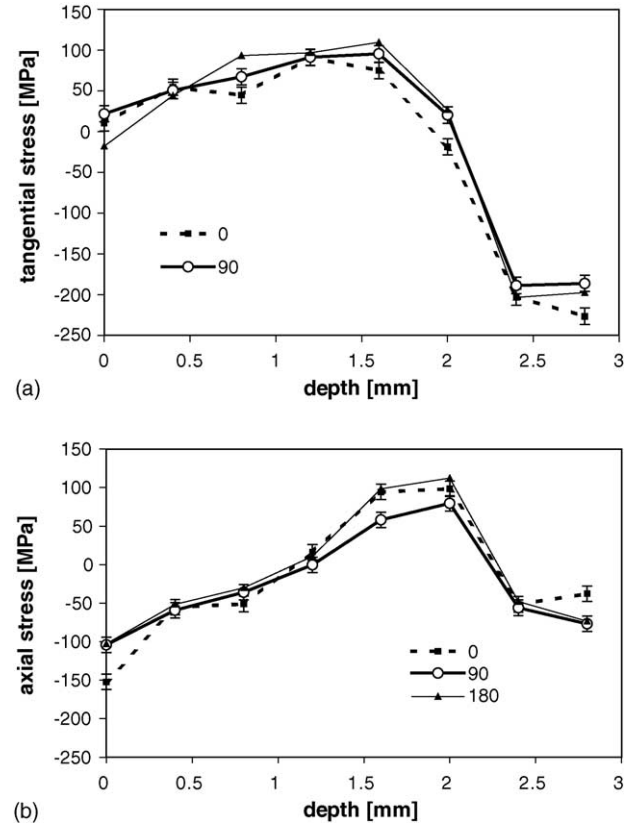

Fig. 6. Tangential (a) and axial (b) stresses in the intact mid-ring measured at positions (0°, 90°, 180°; see Fig. 11). The *x*-axis (depth) starts at the outer surface.

3. Results and discussion

The measurements on the rings were made on locations associated with the symmetry of the original blank: the rolling direction, the transverse direction, and the bi-sector lines between RD and TD. The influence of that symmetry is still visible in the profiles of radial deviation in Fig. 3a where local maxima of increased radius are visible along TD (45° and 225°), and along RD (135° and 315°). Minima are found at the bi-sector positions. However, the comparison of Fig. 3a and the thickness profiles in Fig. 3b shows that the maxima and minima of the radial deviation do not coincide with those of the thickness profiles in Fig. 3b, hence the radial deviation is more of an indicator for a radial shape distortion and it does not allow conclusions about thickness variations.

There is a direct link between the wall thickness and the accumulated plastic strain because any variation from the original thickness of the blank is the result of a plastic flow of material both in the axial direction and around the circumference. One way of characterizing forming strains is the *R*-value, i.e. the ratio of the width-strain in the in-plane direction perpendicular to the applied stress to the thickness strain (ND direction), also perpendicular to the applied stress. From the tensile samples we found $\varepsilon_{RD}/\varepsilon_{ND} = 1.50$ for a 33% strain in the RD direction, and $\varepsilon_{RD}/\varepsilon_{ND} = 1.88$ for a 36% strain in the TD direction. However, we do not find the 180° (RD–TD–RD–TD) symmetry in the thickness profile of the cup wall. The absence of the symmetry of the original blank in the wall thickness was consistently found also in other cups, and it can be attributed to variations of the blankholder force as well as friction.

Overall, the circumferential thickness differences are <3%, which is small compared to the decrease in thickness

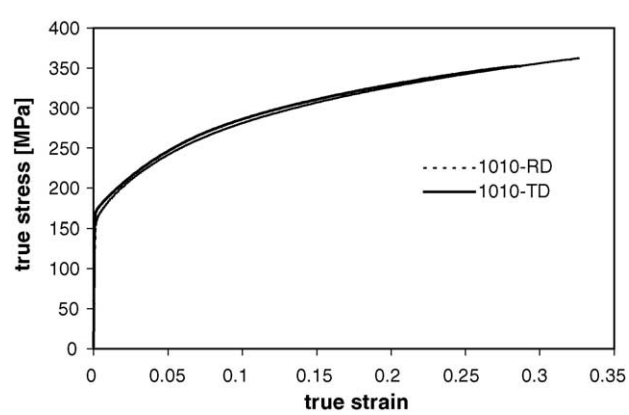

Fig. 7. Stress–strain curve for specimens cut from the original blank in the RD and TD directions.

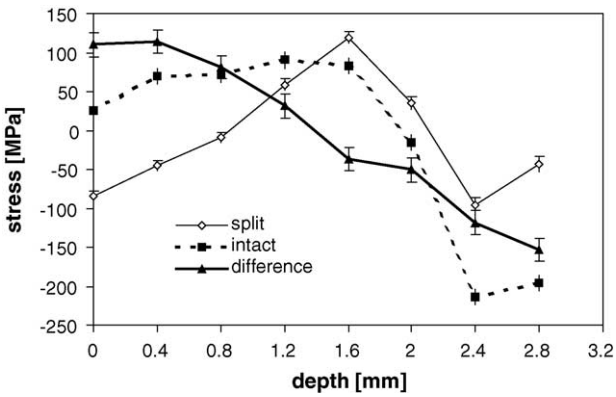

Fig. 8. Average stresses for the intact and split mid-ring and their difference. The *x*-axis (depth) starts at the outer surface.

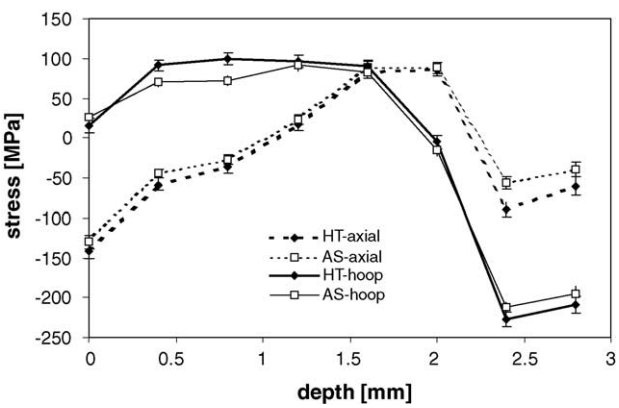

Fig. 9. Comparison of stresses in the cups made from the annealed blank (HT) and made from the as rolled blank (AS). The *x*-axis (depth) starts at the outer surface.

from the top-ring to the bottom-ring (≈10%). As a result, the overall variations of plastic strain are much bigger in the axial direction than around the circumference. The effect of overall increased plastic strain magnitudes is that the strain coordinates of every location for a given axial coordinate are moved

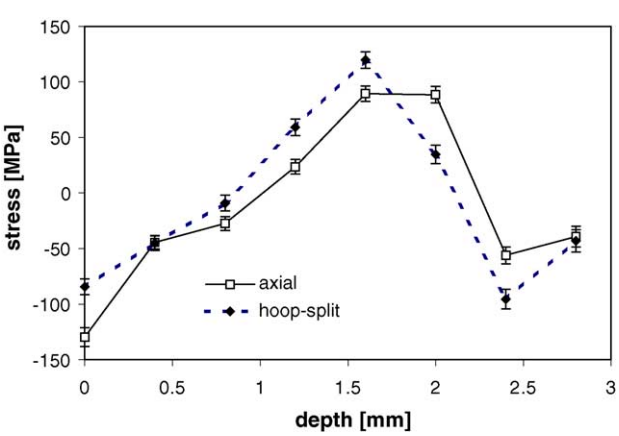

Fig. 10. Average axial and tangential stresses in the split ring. The *x*-axis (depth) starts at the outer surface.

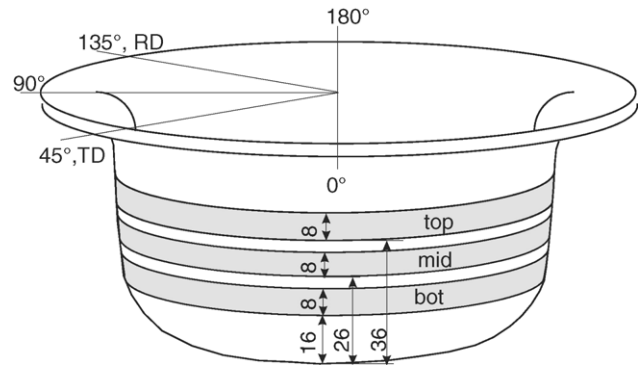

Fig. 11. Schematic of the cup with the locations of the rings. The rolling direction (RD) and the transverse direction (TD) of the initial blank are indicated.

to higher values in the stress–strain curve. The stress–strain curve becomes increasingly flat in the plastic region, thus reducing the possible stress differences between points in the cup wall that have different magnitudes of true strain. This effect is analogous to a stress relief by a homogeneous plastic deformation.

Consequently, stress magnitudes decrease together with the thickness towards the cup bottom. This is well reflected both for the tangential stresses and axial stresses in the intact top, middle and bottom rings in Fig. 4 showing that the residual stresses become increasingly flat towards the cup bottom. The axial stresses are affected more strongly because the true strain increases in the axial direction.

Around the circumference the stress variations for different specimen directions are small with the most notable differences occuring between the RD and TD directions (Figs. 5 and 6). The positions (0°, 90° and 180°) are bi-sector directions that are equivalent with respect to the symmetry of the blank. In Fig. 5, the difference between maximum and minimum stresses is slightly smaller in the TD direction which points towards an increased level of plastic strain. However, there is no obvious correlation to the thickness profile, and, as shown in Fig. 7, the similar tensile properties along RD and TD give no indication of strength related effects.

Other possible explanations are different grain–grain interaction stresses due to grain orientation dependent yield points in the RD and TD directions, and differences in the local elastic constants. Both effects are correlated through preferred grain orientation, which is different in both directions. The in-plane elastic anisotropy of the initial blank is <5% and it was neglected in the stress calculations. However, the deep drawing produces substantial changes of the grain orientations (Fig. 2), which is currently under further investigation.

The split ring test is one of the most common springback measurements, in which the opening of the split mid-ring is measured. It also offers an opportunity to evaluate the quality of the residual stress measurements by comparing

Table 1
Measured and calculated ring openings

	Top	Middle	Bottom
Measured opening (mm)	12.9 (2)	10.4 (2)	7.4 (2)
Calculated (mm)	–	11.8 (4)	–

the measured opening to the numerical value calculated from the measured stresses. If anelastic effects (non-elastic recovery strains) are disregarded then the through-thickness stress change is a linear function of the depth. The stress change together with the stresses in the intact and the split ring is shown in Fig. 8. The observed stress change is linear to a good approximation. The procedure for calculating the ring opening from the stress change is described in [7]; here we list in Table 1 only the measured openings for the three rings and the calculated opening for the mid-ring.

The agreement between measurement and calculation is reasonably good, considering that the averages are taken only over one half of the rings at the positions (0°, 45°, 90°, 135° and 180°). As an effect of the large thickness, the springback is comparatively small.

The effect of the stress relief in the blank on the residual stresses in the ring is shown in Fig. 9. The stresses are virtually identical, thus indicating the negligible effect of the initial coldwork on the springback.

Some insight into the stresses in the intact cup before cutting can be obtained by comparing the average axial and tangential stresses in the split ring in which the springback has already taken place both in the tangential and in the axial direction as shown in Fig. 10.

The operation of cutting the cup into rings induces axial recovery, i.e. after cutting, each ring is in the axially unloaded state and there is both stress balance ($\int \sigma_{ax}\,\mathrm{d}A = 0$, where A is the wall cross section) and balance of the bending moment ($\int \sigma_{ax}\,z\,\mathrm{d}z = 0$, where z is the thickness coordinate).

After splitting the ring, the same applies to the tangential stresses. The ring is in the unloaded state in both directions, and as a consequence, both stress distributions become very similar. Their characteristic shape is caused by a sequence of bending at the die radius and unbending at the punch radius. At a more detailed level, the stresses depend on the specific combination of forming parameters for the deep drawing operation, specifically on the depth of the cup, the cup diameter and on the bending radii of the tooling. An increased depth of the cup increases homogeneous stretching which 'flattens' the tangential stresses and, even more so, the axial stress distributions (Fig. 4). A decreased bending radius of the tooling can cause excessive strains on both sides, thus actually reducing springback at an increased risk of cracking on the outside.

Data for a direct analysis of the effect of the bending radius are not available. However, there are some results from a previous work [7] on an Al-6022 cup with the same forming parameters but with lower wall thickness of 0.92 mm for which the ratio of bending radius (ring radius for tangential stresses) to thickness is three times smaller. The stress–strain curves of Al-6022 and AISI-1010 are very similar which enables a direct comparison as shown in Fig. 12.

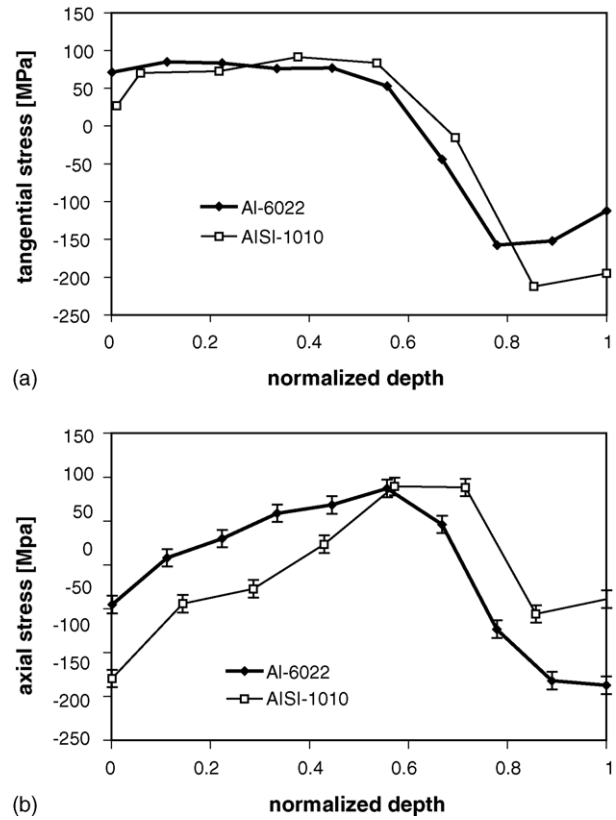

Fig. 12. Average tangential (a) and axial (b) stresses in the intact mid-rings of an AISI-1010 cup and an Al-6022 cup. The x-axis (depth) starts at the outer surface.

For the tangential stresses, the only notable dissimilarities appear close to the inner surface because here the magnitude of the true strain increases faster with the thickness coordinate in compression than in tension. Here, the bending radius is the diameter of the cup, and the ratio of radius to thickness is large for both Al-6022 and AISI-1010.

The differences become larger for the axial stresses where the bending radius is only 10 mm compared to sheet thicknesses of 3 and 1 mm, respectively. In the case of AISI-1010 cup the thickness effect becomes visible, and both for axial and tangential stresses the neutral plane is shifted towards the inside, which is consistent with predictions from plastic bending theory.

4. Conclusions

Overall, both tangential and axial stress distributions exhibit the general features characteristic for the plastic bending of a material with work hardening. At a more detailed level, the stresses are generally non-symmetric with respect to the neutral plane which generally appears to be shifted towards the inner surface as a result of higher true strains on the inside

of the cup. The true strains are also higher towards the cup bottom due to increased stretching which acts as a stress relief and it reduces stress magnitudes. The circumferential variations of both axial and hoop stresses appear to be associated with the RD/TD symmetry of the original blank. The thickness effect points out the influence of the ratio of bending radius to thickness which, for small values of the ratio, can produce large changes in the stress with smaller springback due to higher true strain magnitudes. A heat treatment of the blank material has no visible effect on the stress distributions.

Acknowledgement

The authors wish to thank Dr. Vladimir Luzin for providing the estimate of the elastic anisotropy of the original blank.

References

[1] J. Danckert, Ann. CIRP 43 (1994) 249.
[2] K. Saito, Y. Shimahashi, in: H. Lippman (Ed.), Proceedings of the Conference on Metal Forming Plasticity, Tutzing, Germany, August 1978, Springer-Verlag, Berlin, 1979, p. 53.
[3] K. Lange, L. Bruckner, Trans. NAMRI/SME (1990) 71.
[4] Y. Yuying, L. Chunfeng, X. Hongzhi, J. Mater. Process. Technol. 30 (1992) 167.
[5] M.S. Ragab, H.Z. Orban, J. Mater. Process. Technol. 99 (2000) 54.
[6] F. Morestin, M. Boivin, C. Silva, J. Mater. Process. Technol. 56 (1996) 619.
[7] T. Gnaeupel-Herold, H.J. Prask, R.J. Fields, T.J. Foecke, Z.C. Xia, U. Lienert, Mater. Sci. Eng. A 366 (2004) 104–113.
[8] T. Foecke, S.W. Banovic, R.J. Fields, J. Miner., Met. Mater. Soc. 53 (2) (2001) 27–30.
[9] R.W. Cahn, P. Haasen (Eds.), Physical Metallurgy, Part II, North-Holland Physics Publishing, New York, 1983.
[10] F. Bollenrath, V. Hauk, E.H. Müller, Z. Metallk. 58 (1) (1967) 76–82.